Bulletin of Mathematical Biology (2007) 69: 861–885
DOI 10.1007/s11538-006-9167-8

ORIGINAL ARTICLE

The Dynamics of Size-at-Age Variability

William S.C. Gurney[a,b,*], A. Roy Veitch[a]

[a] *Department of Statistics and Modelling Science, University of Strathclyde, Glasgow G1 1XH, Scotland*
[b] *F.R.S. Marine Laboratory, Aberdeen, Scotland*

Received: 27 November 2005 / Accepted: 6 September 2006 / Published online: 20 January 2007

Abstract In this paper, we propose a theoretical framework within which a unified treatment of the key sources of size-at-age variability—size dependence of growth rate, stochastic growth rate variations and individual-to-individual variability in growth performance—is possible. We use this framework to develop a general criterion for growth depensation in cohorts, which we define as the increase of the coefficient of variation of size-at-age, with increasing age. We use this criterion to show that size dependence of growth rate, acting alone, is depensatory only if the growth rate increases faster than linearly with size (that is, if growth is faster than exponential), while stochastic growth rate variation is invariably depensatory. Many species exhibit growth rates that scale less than linearly with size; indeed the commonly used von Bertalanffy model shows growth rates which actually decrease with size. In such a species, the size dependence of growth rate acts compensatorily, while stochastic growth rate variability is depensatory. We show that the tension between these two mechanisms leads to quasi-stationary size-at-age variability, which we can calculate analytically in some special cases and obtain by a simple numerical procedure where analysis is impractical.

Keywords Size-at-age variation · Growth rate variability

1. Introduction

Because all animals age at the same rate, understanding changes in population age-structure is a relatively straightforward book-keeping exercise. In contrast, the high variability in somatic growth rates, even between apparently similar individuals (Sebens, 1987; Pfister and Peacor, 2003), makes understanding population size-structure a much more challenging exercise. A comprehensive theory of the dynamics of population size structure remains one of the key challenges for ecological theory.

*Corresponding author.
E-mail address: bill@stams.strath.ac.uk (William S.C. Gurney)

The importance of meeting this challenge is emphasised by the key role size-structure plays in many ecological and management issues. In exploited populations subject to size-dependent exploitation (such as fisheries), changes in size structure (of either anthropogenic or natural origin) can have significant economic as well as ecological impacts (Rose, 2004). In unexploited populations, size structure can still be an important determinant of population dynamics; mediating average population fecundity (Marteinsdottir and Begg, 2002), intraspecific interactions such as cannibalism (DeAngelis et al., 1979; Brunkow and Collins, 1998) and interspecific interactions such as predation (Wootton, 1992).

Increases in size variability with time or age are often referred to as 'growth depensation' while decreases are termed 'growth compensation' (Ricker, 1958). Pfister and Stevens (2002) have identified the three classes of mechanism that can lead to growth depensation as: systematic size dependence of growth rate, individual-to-individual growth rate variation consequent upon environmental, behavioural or genetic differences, and stochastic variation of individual growth performance, which is uncorrelated with that of other population members.

The first of two of these classes are the most amenable to analysis and have thus been the subject of most previous work (e.g. DeAngelis and Huston, 1987; de Roos et al., 1992; Pfister and Peacor, 2003). Stochastic variations of individual growth performance complicate analysis considerably, and their obvious importance in determining size dispersion in many real populations has led to arguments (e.g. Pfister and Stevens, 2002; Fujiwara et al., 2004, 2005) that explicit individual by individual representations are the most fruitful route to a full understanding of growth depensation. However, the possibility of using a more analytic approach is suggested by the work of Bardos (2005) who describes the application of a probabilistic variant of the Gompertz growth model (Gompertz, 1825) to the analysis of size-increment data in abalone.

In this paper, we describe an analytic framework that allows integrated discussion of the dynamics of size-at-age dispersion. We use this framework to derive a general criterion for the occurrence of growth depensation, which we use to identify the shapes of deterministic growth trajectories that lead to amplification or attenuation of size variation at recruitment, and to show that very narrow size at recruitment distributions always show initial growth depensation under stochastic growth rate variation.

We illustrate the utility of our results by investigating size dispersal in a population showing von Bertalanffy growth with randomly varying growth rates. We find that the compensatory tendency of this mode of deterministic growth, combined with the depensation inherent in random growth rate variations, produces an initial-condition-independent trajectory of the size-at-age coefficient of variation (c.v.) that we can estimate analytically. We demonstrate the accuracy of this estimate, together with the (rather small) effects of size-dependent mortality, by comparison with simulation results.

2. Individuals and populations

We envisage a population as being made up of 'families' each comprising a set of individuals characterised by age a and some measure of size or development,

which, since weight is one of the more obvious choices of metric, we denote by w. We represent the rate of change of the size measure for an individual in family i of age a and size w by a function g_i, which we henceforth refer to as the 'development rate.' Families also share the same functional relationship between age, size and mortality. The definition of family is perhaps most easily understood in terms of genetically determined characteristics. The formalism might also be used to differentiate between groups of genetically unrelated individuals exhibiting systematic differences in the size dependence of growth or mortality due to environmental or behavioural differences.

Changes in development rate with time and differences between individuals in a single family are characterised by variations in the value of a single parameter γ. That is, at every time, each individual in family i has a value of γ_i drawn from a family-specific statistical distribution. Thus, the two quantities which characterise the state of an individual in family i change with time according to

$$\frac{\mathrm{d}a}{\mathrm{d}t} = 1, \qquad \frac{\mathrm{d}w}{\mathrm{d}t} = g_i(a, w, \gamma_i). \tag{1}$$

For example, later in the paper, we discuss a population composed of a single family, which exhibits von Bertalanffy growth. Here, the size metric is normalised body length (which, for consistency with the general literature, we denote by L) and we show in Appendix D that the rate of change of L is related to its current value and the normalised assimilation rate u, by $g = [u - L]^+$ where $[x]^+ = \max(0, x)$. We shall identify the assimilation rate u as our varying parameter (i.e. γ) and assume its variations to be random.

We would expect to describe the status of family i at time t by counting the number of individuals with age a and size w. However, if variations in γ (and hence in g) are random, this count is itself a random variable that we can only describe by a probability density function $P_i(n, a, w, t)$ defined so that

$$P_i(n, w, a, t)\,\mathrm{d}n\,\mathrm{d}w\,\mathrm{d}a = \left\{ \begin{array}{l} \text{Probability that } n \to n + \mathrm{d}n \text{ individuals} \\ \text{in family } i \text{ have weight in } w \to w + \mathrm{d}w \\ \text{and age in } a \to a + \mathrm{d}a \text{ at time } t \end{array} \right\}. \tag{2}$$

To proceed further we need more detail about the nature of the variability in γ_i. Our first assumption will be that all members of a single family exhibit variations with the same statistical characteristics. Second, we assume that variations in development rate for individuals in family i arise from white (i.e. temporally uncorrelated) variations in γ_i, which result in an expected development rate $\overline{g_i}(a, w)$ and (white noise) variations about that expected rate characterised by a power spectral density $2D_i(a, w)$.

In Appendix A, we show that under these assumptions the probability density function for the family age-size distribution must obey the conservation equation

$$\frac{\partial P_i}{\partial t} + \frac{\partial P_i}{\partial a} + \frac{\partial}{\partial n}\left[-m_i n P_i\right] + \frac{\partial}{\partial w}\left[\overline{g_i} P_i - D_i \frac{\partial P_i}{\partial w}\right] = 0 \tag{3}$$

where m_i represents the (age and size-dependent) per capita mortality rate for family i.

Although a full description of family i's age-size dynamics requires us to define the probability density function P_i, we seldom have data that would allow us to estimate it. If our data comprises observations of a single population, then our best estimate of the size-at-age distribution we should observe is the expected number density of individuals in family i of size w at age a, which is related to P_i by

$$n_i(a, w, t) = \int_0^\infty n P_i(n, a, w, t)\, \mathrm{d}n. \tag{4}$$

Provided that the mortality function, m_i, is not an explicit function of n_i, it is straightforward to show from Eq. (3) that the conservation equation for n_i is

$$\frac{\partial n_i}{\partial t} + \frac{\partial n_i}{\partial a} + \frac{\partial}{\partial w}\left[\overline{g_i} n_i - D_i \frac{\partial n_i}{\partial w}\right] + m_i n_i = 0. \tag{5}$$

This dynamic equation is a natural extension of the McKendrick-von Foerster equation (von Foerster, 1959) describing the deterministic growth of an age-size structured population. Like its deterministic progenitor, it must be solved subject to a condition at the age-zero boundary that describes the rate of recruitment of new-born individuals. If the expected rate of recruitment of family i newborns with sizes in $w \to w + \mathrm{d}w$ at time t is $R_i(w, t)\, \mathrm{d}w$ then (recalling that $\mathrm{d}a/\mathrm{d}t = 1$) we require that

$$n_i(0, w, t) = R_i(w, t). \tag{6}$$

In some applications (for example, the model of irreversible von Bertalanffy growth considered later, in which w is identified with the normalised length L), the individual development rate g is constrained to be positive. Under these circumstances, a consistent determination of the age-size distribution function n_i must show the low L side of the distribution either stationary or moving towards higher L. Inspection of Eq. (5) shows that this cannot be unequivocally true, since a large enough positive L-gradient, accompanied by a small enough n_i, will always cause the net L-flux (the term in square brackets in Eq. (5)) to be negative.

To assess the seriousness of this problem, in Fig. 1, we compare the size-at-age distributions for a single cohort exhibiting irreversible von Bertalanffy growth predicted by numerical solutions of Eq. (5) with distributions obtained from ensembles of 10,000 individual-by-individual simulations. In all the cases discussed later in the paper, we found essentially perfect agreement. Experiments under deliberately extreme conditons generated detectable errors, but only at the level of a few percent.

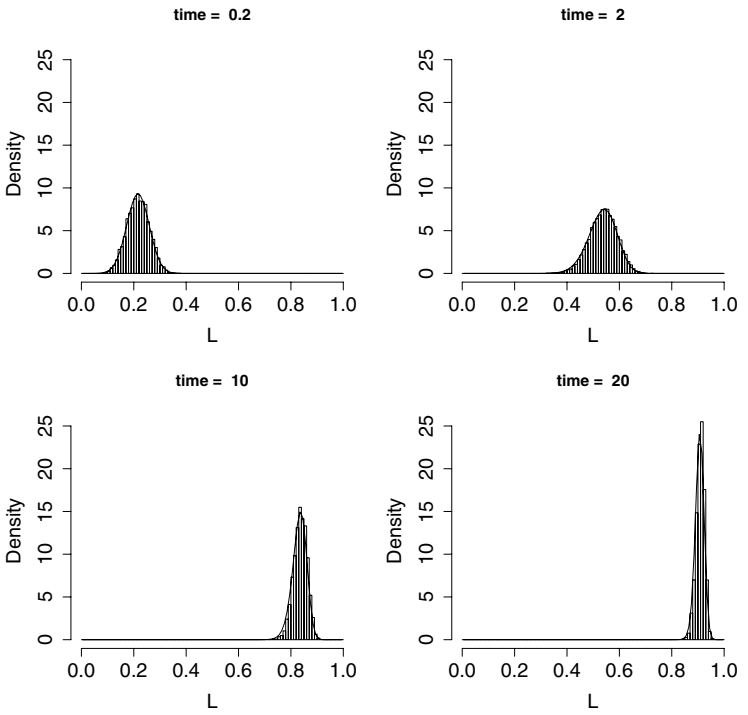

Fig. 1 Comparison of solutions of Eq. (5) with probability density functions estimated from explicit simulations ($\mathrm{d}t = 0.1$) of 10,000 individuals exhibiting ireversible von Bertalanffy growth (see Appendix D) growing over 20 normalised time units with randomly varying growth rates uniformly distributed over [0, 1]. and a gaussian initial distibution with mean 0.1 and S.D. = 0.03.

3. Population statistics

Although the expected size-at-age distribution for individual families is in principle observable, the practical obstacles are formidable. Even if the 'family' is wholly defined by genetics, assignment of individuals to families is expensive and time-consuming. Size measurements are generally straightforward, but unambiguous determination of age often requires microscopic examination of body structures such as scales or otoliths. In practice, we are likely to possess only enough data to define summary statistics (such as the mean and variance) for the size of all individuals of a given age in the population.

The key step in relating these population-level statistics to the set of family expected size-at-age distributions is to define the moments (about the origin) of the population size-at-age distribution. We denote the qth moment by W_q and recognise that the moments of the population distribution are just the sum of the moments of the family distributions. Hence

$$W_q(a,t) = \sum_{\text{all } i} \int_0^\infty w^q n_i(a,w,t)\,\mathrm{d}w. \tag{7}$$

Once we know the moments, we can easily calculate the mean and variance of size-at-age, which we write as $\widehat{w}(a,t)$ and $v_w(a,t)$, from

$$\widehat{w}(a,t) = \frac{W_1}{W_0}, \qquad v_w(a,t) = \frac{W_2}{W_0} - \left(\frac{W_1}{W_0}\right)^2. \tag{8}$$

For future convenience, we define two further quantities—the mean age-specific development rate

$$\widehat{g}(a,t) = \frac{1}{W_0}\sum_{\text{all } i}\int_0^\infty \overline{g_i} n_i \,\mathrm{d}w \tag{9}$$

and the covariance of size and development rate for individuals of age a,

$$c_{wg}(a,t) = \left[\frac{1}{W_0}\sum_{\text{all } i}\int_0^\infty w_i \overline{g_i} n_i \,\mathrm{d}w\right] - \widehat{w}\widehat{g}. \tag{10}$$

Our principal aim in this paper is to understand the changes in variability that occur as cohorts of individuals develop though their life-cycle. We thus wish to compare the variability of groups of individuals whose mean size differs by as much as several orders of magnitude. The natural statistic to use in this enterprise would be the coefficient of variation (the ratio of the standard deviation to the mean), but in the the interests of algebraic simplicity, we shall use the square of the coefficient of variation (c.v.), which we call the relative variance (r.v.), $V_w \equiv v_w/\widehat{w}^2$. This quantity is related to the moments by

$$V_w(a,t) = \left[\frac{W_2 W_0}{W_1^2} - 1\right]. \tag{11}$$

4. Age dependence of size-variability

In general, the family distributions that underlie our summary statistics will undergo complex changes with age and time, reflecting growth, mortality and recruitment. For the sake of simplicity, we consider a situation in which new-borns are recruited to the population at a constant rate and grow thereafter in a statistically stationary environment. Under these circumstances, we normally expect the population age-size distribution to converge to a stationary (time-independent) form, which we write as $n_i^*(a,w)$. In this case the population statistics will take time-independent forms that we denote by $W_q^*(a)$, $\widehat{w}^*(a)$, $v_w^*(a)$, $\widehat{g}^*(a)$, $c_{wg}^*(a)$ and $V_w^*(a)$. Substituting steady state quantities into Eq. (11) and differentiating with respect to age shows that

$$\frac{\mathrm{d}V_w^*}{\mathrm{d}a} = \left(\frac{W_0^* W_2^*}{[W_1^*]^2}\right)\left(\frac{1}{W_2^*}\frac{\mathrm{d}W_2^*}{\mathrm{d}a} - \frac{2}{W_1^*}\frac{\mathrm{d}W_1^*}{\mathrm{d}a} + \frac{1}{W_0^*}\frac{\mathrm{d}W_0^*}{\mathrm{d}a}\right). \tag{12}$$

Equation (12) also describes a somewhat different situation that will be our primary concern for the remainder of this paper, namely the growth of a single cohort all of whose members are aged zero at some initial time (say $t = 0$) and to which no further recruitment takes place. In this case, we interpret $n_i^*(a, w)$ as the size distribution of those family i individuals who are still alive at age a.

Differentiating Eq. (7) with respect to a tells us that at the stationary state, the rate of change of the qth moment of the population size-at-age distribution with age is

$$\frac{\mathrm{d}W_q^*(a)}{\mathrm{d}a} = \sum_{\text{all } i} \int_0^\infty w^q \frac{\partial n_i^*(a, w)}{\partial a} \, \mathrm{d}w. \tag{13}$$

Using Eq. (5) to relate the partial derivative of each family size-at-age distribution to its growth and mortality functions allows us to rewrite this as

$$\frac{\mathrm{d}W_q^*(a)}{\mathrm{d}a} = \sum_{\text{all } i} \int_0^\infty w^q \left[-\frac{\partial}{\partial w} \left(\overline{g_i} n_i^* - D_i \frac{\partial n_i^*}{\partial w} \right) - m_i n_i^* \right] \mathrm{d}w. \tag{14}$$

Integrating Eq. (14) by parts shows that provided $n_i^* \to 0$ sufficiently fast as $w \to 0$ and $w \to \infty$

$$\frac{\mathrm{d}W_q}{\mathrm{d}a} = G_q^* - M_q^* \tag{15}$$

where

$$G_q^* = \begin{cases} \displaystyle\sum_{\text{all } i} \int_0^\infty \left[q w^{q-1} \overline{g_i} + \frac{\partial}{\partial w} \left(q w^{q-1} D_i \right) \right] n_i^* \, \mathrm{d}w, & \text{if } q > 0 \\ 0, & \text{otherwise} \end{cases} \tag{16}$$

and

$$M_q^* = \sum_{\text{all } i} \int_0^\infty w^q m_i n_i^* \, \mathrm{d}w. \tag{17}$$

Substituting Eq. (15) into (12) shows that the rate of change with age of the r.v. for the population size-at-age distribution is

$$\frac{\mathrm{d}V_w^*}{\mathrm{d}a} = \left(\frac{W_0^* W_2^*}{[W_1^*]^2} \right) \left(\frac{G_2^*}{W_2^*} - \frac{2G_1^*}{W_1^*} - \left[\frac{M_2^*}{W_2^*} - \frac{2M_1^*}{W_1^*} + \frac{M_0^*}{W_0^*} \right] \right). \tag{18}$$

We note that the validity of Eqs. (16) and (18) requires that n_i^* goes to zero 'sufficiently fast' as w goes to zero. In the case of exponential growth, 'sufficiently fast' clearly implies 'faster than exponentially.' However no real individual can achieve

infinite size, so a realistic population description must either incorporate an upper growth asymptote, or postulate mortality rates that ensure that no individual survives beyond some (possibly arbitrary) maximum age.

While no sensible initial condition can place significant numbers of newborns at $w = 0$, growth rates that are not constrained to be positive can result in (model) individuals with weights that are zero (or even negative!). Although starvation resistance varies greatly between species, individuals of a given species will die with probability 1 as soon as they have lost some critical proportion of their body mass (usually between 50 and 90%). Hence, we can argue that any sensible population description must incorporate a mortality scheme that ensures that $n_i^*(a, 0) = 0$.

Any population description that obeys both of these requirements will ensure the validity of Eqs. (16) and (18) and hence the applicability of the analysis in the remainder of this paper.

5. Size-independent mortality

In the special case where the per-capita mortality rate is given by the same function of age for all families (that is, $m_i = m(a)$ for all i) Eq. (17) implies

$$M_q^* = m \sum_{\text{all } i} \int_0^\infty w^q n_i^* \, \mathrm{d}w = m W_q^*. \tag{19}$$

This, in turn, implies that the term in square brackets in Eq. (18) is identically zero, so the expression for the rate of change of the size-at-age r.v. simplifies to

$$\frac{\mathrm{d}V_w^*}{\mathrm{d}a} = \left(\frac{W_0^* W_2^*}{[W_1^*]^2} \right) \left(\frac{G_2^*}{W_2^*} - \frac{2G_1^*}{W_1^*} \right). \tag{20}$$

This implies that the condition for the size-at-age r.v. to increase with age at the steady state is

$$\frac{G_2^*}{W_2^*} > \frac{2G_1^*}{W_1^*} \tag{21}$$

with a decrease if the inequality is reversed and stasis if the two sides are equal.

5.1. Distinct individuals with constant properties

The first application of the general theory we have just set out is to a population of genetically distinct individuals with size-independent per-capita mortality rate and growth performance that remains constant with time. In the language of the previous discussion, the population consists of N families each containing a single individual with a time-independent development rate formally identical to $\overline{g_i}$. Since the growth rate is time-independent, $D_i = 0$.

Because there is only one individual per 'family,' the expected steady-state family age-size distribution contains one individual whose size-at-age a is exactly w_i. We represent this situation by writing the family age-size distribution as a Dirac delta function ($n_i^*(a, w) = \delta(w - w_i)$).

Since the per-capita mortality rate is size-independent, the condition that the size-at-age r.v. increases with age is given by Eq. (21), which is an inequality. When n_i^* is a delta-function, this can be rewritten as

$$\frac{\sum_i w_i g_i(w_i)}{\sum_i w_i^2} > \frac{\sum_i g_i(w_i)}{\sum_i w_i}. \tag{22}$$

Comparison of the components of this inequality with the population statistics defined in Eqs. (8)–(10) shows that it can be rewritten as

$$c_{wg}^* > \left(\frac{\widehat{g}^*}{\widehat{w}^*}\right) v_w^*(a). \tag{23}$$

Thus, in this special case, the size-at-age r.v. increases with age if and only if the correlation of size and growth rate is large enough compared to the variance of w.

We now make an additional simplifying assumption, namely that the development process is allometric, so that $g_i = \alpha_i w^\beta$, where α_i is a time-independent scaling parameter that varies between individuals and β is an allometric power that is constant across the population. With this assumption, and after some algebraic manipulation, we can rewrite the condition for the steady state size-at-age r.v. to increase with age, (Eq. 21), which is an inequality, as

$$\sum_i \sum_j \left[\alpha_i w_i^{\beta+1} w_j - \alpha_j w_j^\beta w_i^2\right] > 0, \tag{24}$$

which (as we show in appendix B) can be re-written in the form

$$\sum_i \sum_{j<i} \left[w_i w_j (w_i - w_j)\left(\alpha_i w_i^{\beta-1} - \alpha_j w_j^{\beta-1}\right)\right] > 0. \tag{25}$$

We now assume that we have arranged the list of families in weight order so that $w_i > w_j$ for all $i > j$. In the special case of identical individuals ($\alpha_i = \alpha$ for all i) we see that Eq. (24), which is an inequality, is guaranteed to be true if and only if $\beta > 1$. This tells us that recruitment size variations of a group of identical individuals will be amplified by subsequent development if development is faster than exponential and will be attenuated if growth is slower than exponential.

Where there is individual variability ($\alpha_i \neq \alpha_j$), the position is more complex. If α is positively correlated with w, then ordering individuals by weight also orders them by α, and $\beta > 1$ guarantees that Eq. (25), which is an inequality, is true. However, $\beta < 1$ no longer guarantees that Eq. (25) is false. Where there is no size variability at recruitment, it is easy to see that Eq. (25) is always true for linear growth ($\beta = 0$) and we conjecture (supported by a number of numerical experiments) that

it is true for all $\beta > 0$. This would be consistent with the intuitively obvious statement that a group of initially identical individuals growing allometrically with differing development rates will show steadily increasing size variability.

5.2. One family with randomly varying development

We next consider a population of genetically identical individuals (a single family) with size-independent per-capita mortality and development rates that vary randomly and independently with time and between individuals, so that

$$g(a, w) = \overline{g}(w) + \gamma(t) \tag{26}$$

where $\gamma(t)$ is a white noise with mean zero and power spectral density $2D$.

In this case, the condition for the size-at-age r.v. to increase with age, i.e. Eq. (21), which is an inequality, can, after substitutions from Eqs. (8)–(10) followed by a little algebraic manipulation, be written as

$$c^*_{wg} > \frac{\widehat{g}}{\widehat{w}} v_w - D. \tag{27}$$

As in the previous special case (c.f Eq. 23, which is an inequality), this shows that the size-at-age r.v increases with age if the covariance of size and development rate is large enough. However, here we also see that increasing D, makes this inequality easier to satisfy, and sufficiently large D guarantees that it must be satisfied for any non-negative c^*_{wg}.

We now repeat the restrictive assumption used in the above discussion of individuals with time-independent demographic properties, namely that the deterministic part of the growth process is allometric so that $\overline{g} = \alpha w^{\beta}$. Under this assumption, the condition that the size-at-age r.v. increases with age can be written as

$$\int_0^\infty \int_0^\infty \left[\alpha w^{\beta+1} x + Dx - \alpha w^{\beta} x^2\right] n^*(a, w) n^*(a, x)\, \mathrm{d}w\, \mathrm{d}x > 0, \tag{28}$$

which (see Appendix C) can be re-written in the form

$$\int_0^\infty \int_0^x \Psi(w, x) n^*(a, w) n^*(a, x)\, \mathrm{d}w\, \mathrm{d}x > 0 \tag{29}$$

where

$$\Psi(w, x) \equiv \alpha w x (x - w)(x^{\beta-1} - w^{\beta-1}) + D(x + w). \tag{30}$$

Clearly $\beta > 1$ guarantees that Ψ is non-negative for all $w < x$, so allometric growth with an allometric constant greater than 1 (that is growth that is faster than exponential) will cause the size-at-age relative variance to increase with age whatever

the random variability in individual development rates. Equally clearly, growth rate variability will increase the rate at which V_w increases with age.

In the special case of exponential growth, $\beta = 1$, we note that if $D = 0$ then $\Psi = 0$ for all $w < x$, but if $D > 0$, then $\Psi > 0$ for all $w < x$. Thus, pure exponential growth, which, in the absence of growth rate fluctuations, exactly maintains the size at recruitment r.v. throughout development, produces steadily increasing V_w if individual development rates fluctuate.

6. Size-dependent mortality

Equation (18) shows that if the mortality rate is size-dependent, the condition for the stationary size-at-age r.v. to increase with age is

$$\frac{G_2^*}{W_2^*} > \frac{2G_1^*}{W_1^*} + \mu, \quad \text{where} \quad \mu \equiv \frac{M_2^*}{W_2^*} - \frac{2M_1^*}{W_1^*} + \frac{M_0^*}{W_0^*}. \tag{31}$$

We consider the special case where all families have the same size-dependent mortality rate $m_i(w) = m_0 + \kappa w$. In this case, Eqs. (17) and (7) show us that

$$\mu = \kappa \left[\frac{\widehat{w^3}}{\widehat{w^2}} - 2\frac{\widehat{w^2}}{\widehat{w}} + \widehat{w} \right]. \tag{32}$$

We now recall that the second and third moments of the size-at-age distribution obey $\widehat{w^2} = (\widehat{w})^2 + v_w$ and $\widehat{w^3} = (\widehat{w})^3 + 3v_w\widehat{w} + v_w\sqrt{v_w}S$, where S is the skewness coefficient. Hence, after some algebraic manipulation we can write μ as

$$\mu = -\kappa \left[\frac{v_w\sqrt{v_w}}{\widehat{w}} \right] \left[\frac{2\sqrt{v_w} - \widehat{w}S}{(\widehat{w})^2 + v_w} \right]. \tag{33}$$

If μ is positive, it increases the R.H.S. of Eq. (31), which is an inequality, thus decreasing the propensity of the size-at-age r.v. to increase with age, with the reverse being true if $\mu < 0$. So long as

$$S < 2\sqrt{(V_w)} = \frac{2\sqrt{v_w}}{\widehat{w}} \tag{34}$$

then μ has the opposite sign to κ, with the opposite being true if the inequality is reversed. This implies that, so long as the size-at-age distribution is not too positively skewed, mortality which increases with age tends to increase size-at-age dispersion, with the reverse being true if mortality decreases with age.

7. Irreversible von Bertalanffy growth

As an application of the body of theory developed in the foregoing part of this paper, we now consider a population of genetically identical organisms (a single

family) exhibiting von Bertalanffy growth (von Bertalanffy, 1938) with a randomly varying feeding rate. In Appendix D, we show that under an appropriate scaling this model can be expressed as

$$g(L,u) = [u - L]^+, \tag{35}$$

where L is the normalised body length, u is the normalised assimilation rate, and $[x]^+ = \max(0, x)$.

To describe the variability in the normalised assimilation rate u, we consider repeated evaluations averaged over $2\tau_m$ normalised time units and express the result as a probability density function $\phi(u)$. As a strategic approximation, we assume that u is uniformly distributed between $1-\alpha$ and 1. That is,

$$\phi(u) = \begin{cases} \alpha^{-1}, & \text{if } 1-\alpha \le u \le 1 \\ 0, & \text{otherwise.} \end{cases} \tag{36}$$

We note from Eq. (35) that an individual of normalised length L experiences zero growth unless u exceeds L. Thus, when we evaluate the expected growth rate $\overline{g}$, we count the growth rate as $u - L$ only for $u > L$ and as zero for all $u < L$. Hence $\overline{g}$ becomes an integral over all possible values of u, greater than L, thus giving

$$\overline{g} = \frac{1}{\alpha} \int_{\max(L,1-\alpha)}^{1} [x - L]^+ \, \mathrm{d}x. \tag{37}$$

Evaluating this integral leads to

$$\overline{g} = \begin{cases} (1-\alpha/2) - L, & L < 1-\alpha \\ (1-L)^2/2\alpha, & 1-\alpha \le L < 1 \\ 0, & L \ge 1 \end{cases}. \tag{38}$$

Similarly, the power spectral density of the growth rate variation (D) is

$$D = \tau_m(\overline{g^2} - (\overline{g})^2). \tag{39}$$

That is

$$D = \begin{cases} \alpha^2\tau_m/12, & L < 1-\alpha \\ \tau_m(1-L)^3[4\alpha + 3(L-1)]/(12\alpha^2), & 1-\alpha \le L < 1 \\ 0, & L \ge 1 \end{cases} \tag{40}$$

Equations (38) and (40) tell us that the expected growth rate $\overline{g}$ and the diffusion rate D both fall smooothly to zero as L approaches 1 and are identically zero when $L > 1$. This implies that biologically sensible initial size-at-age distributions cannot

contain any individuals with $L > 1$ and that subsequent evolution of the size-at-age distribution cannot result in individuals with $L > 1$.

7.1. Size-independent mortality: analysis for $L < 1 - \alpha$

If the mortality rate is size-independent (that is m depends on age but not size) the condition for the steady state size-at-age variability to increase with age is Eq. (21), which is an inequality. We initially restrict our consideration to the size-at-age distributions for ages such that no individual can have a scaled length exceeding $(1 - \alpha)$. In this case, the key components of Eq. (21), which is an inequality, are

$$G_1^* = \int_0^{1-\alpha} \left[1 - \frac{\alpha}{2} - L\right] n^* \, \mathrm{d}L \tag{41}$$

and

$$G_2^* = 2\int_0^{1-\alpha} \left[L\left(1 - \frac{\alpha}{2} - L\right) + \frac{\alpha^2 \tau_m}{12}\right] n^* \, \mathrm{d}L. \tag{42}$$

When there is no variability in u ($\alpha \to 0$), we can use the methods employed in earlier sections to show that Eq. (21), which is an inequality, can be re-expressed as

$$I \equiv \int_0^{1-\alpha} \int_0^{L} \left[-(L - X)^2\right] n^*(X) n^*(L) \, \mathrm{d}X \mathrm{d}L. > 0. \tag{43}$$

Since the integrand is inevitably negative, this inequality is never true, which clearly shows that with no variability in u the effect of von Bertalanffy growth is to attenuate any pre-existing variability.

Conversely, if n^* is a delta function at (say) the recruitment weight L_R, then it is easy to show that Eq. (21), which is an inequality, reduces to

$$\frac{\alpha^2 \tau_m L_R}{12} > 0, \tag{44}$$

which cannot be false, thus demonstrating that growth rate variability acting alone inevitably causes size-at-age variability to increase with age.

In this model, deterministic growth tends to decrease size-at-age variability and growth rate variability tends to increase it. The latter tendency clearly predominates when the size-at-age distribution is narrow enough, while we might expect the former to dominate when the size-at-age distribution is wide.

To explore this possibility further, we note that whatever the shape of n^*, provided it is confined to the range $L < 1 - \alpha$, we can re-write G_1^* and G_2^* as

$$\frac{G_1^*}{W_0^*} = \left(1 - \frac{\alpha}{2}\right) - \widehat{L}, \qquad \frac{G_2^*}{2W_0^*} = \left(1 - \frac{\alpha}{2}\right)\widehat{L} - \widehat{L^2} + \frac{\alpha^2 \tau_m}{12}. \tag{45}$$

In this case, Eq. (21), which is an inequality, can be re-expressed as

$$V_L^* \equiv \frac{v_L^*}{(\widehat{L})^2} < \frac{\alpha^2 \tau_m}{6\widehat{L}(2-\alpha)}, \tag{46}$$

thus demonstrating that if the relative variance of size at a given age is less than the R.H.S. of Eq. (46), which is an inequality, then it rises, while if it is greater then it falls. This raises the possibility that a given level of growth rate variation implies a quasi-steady state level of size-at-age variability, which we can calculate by replacing Eq. (46), which is an inequality, with an equality. We note that this 'quasi-steady state' relative variance falls in inverse proportion to the mean length, thus implying that tight initial length distributions will give rise to humped trajectories of r.v. against age, while highly dispersed initial length distributions will give rise to monotone decreasing trajectories of size-at-age r.v. against age.

We demonstrate the utility of this insight in Fig. 2 where we show the results of a series of ensembles of 10,000 individual-by-individual simulations. In Fig. 2a we show the size-at-age c.v. (the square root of the size-at-age r.v.) for two ensembles where each individual grows with normalised assimilation rate uniformly distributed between 0.8 and 1. The two ensembles are distinguished only by the width of the initial length distribution, and we see that the delta-function initial distribution produces a humped trajectory of c.v. against age, whereas the wide initial distribution produces a monotone decreasing trajectory.

Even more interestingly, we see that the two trajectories converge extremely quickly, suggesting that the 'tipping point' of Eq. (46), which is an inequality, is a strong attractor. Since the value of c.v implied by this attractor (shown by the dotted line in the figure) clearly decreases as the mean length rises, we are not surprised that the measured values are systematically above the tipping point over the range where we might expect Eq. (46), which is an inequality, to apply ($L_{\max} < 1-\alpha = 0.8$).

7.2. Size-independent mortality: analysis for $L > 1-\alpha$

Given the success of Eq. (46), which is an inequality, we now seek a similar result when the distribution is confined to $L > 1-\alpha$. This turns out to be a much more serious algebraic challenge and we have not been able to obtain an exact result. However, some heroic approximations yield a workable estimate.

We begin by noting that if we neglect terms in $\partial D/\partial L$ on grounds that they are likely to be quite small in comparison with D, then we can write G_1^* and G_2^* for distributions confined to $L > 1-\alpha$ as

$$\frac{G_1^*}{W_0^*} = \frac{1}{2\alpha}(1 - 2\widehat{L} + \widehat{L^2}), \qquad \frac{G_2^*}{W_0^*} = \frac{1}{\alpha}(\widehat{L} - 2\widehat{L^2} + \widehat{L^3}) + 2\widehat{D}. \tag{47}$$

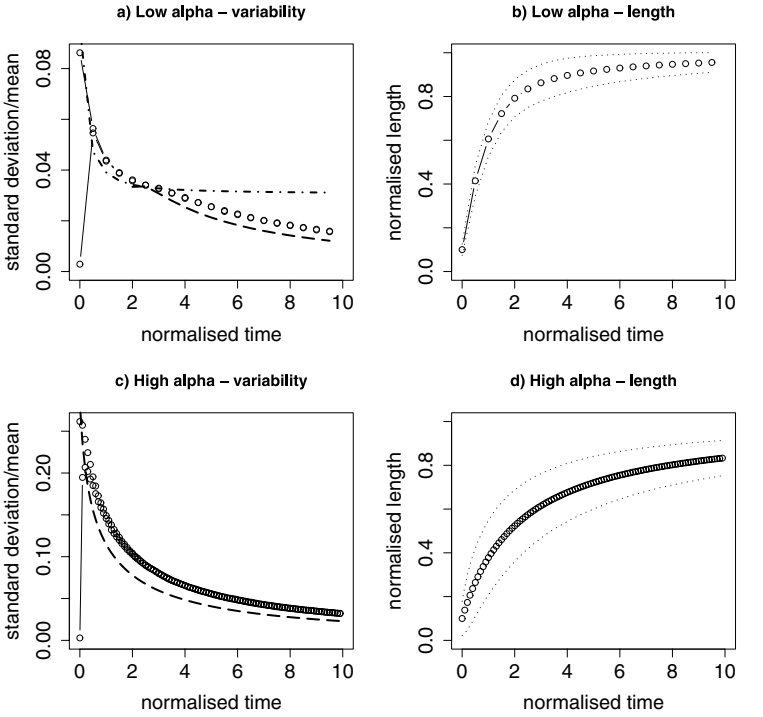

Fig. 2 Simulations of an ensemble of 10,000 individuals growing with randomly varying growth rates. The points in (a) show $\sqrt{V_L}$ against t for two initial conditions with $\alpha = 0.2$ and $\tau_m = 0.25$. One replicate has all individuals the same initial length, while the other has initial lengths spread uniformly between 0.07 and 0.13. (b) shows the mean length $\pm$ 3 S.D. for the same system. The points in (c) show the variability with $\alpha = 1$ and $\tau_m = 0.05$. One replicate has a delta function initial length distribution, while the other has initial lengths spread uniformly between 0.001 and 0.19. (d) shows mean length and mean length $\pm$ 3 S.D. for this simulation. The *dash-dotted* line in (a) shows $\sqrt{V_L}$ defined by the 'tipping point' of Eq. (46), which is an inequality. The *dashed lines* in (a) and (c) show $\sqrt{V_L}$ defined by the tipping point of Eq. (49), which is an inequality.

Recalling that $\widehat{L^2} = (\widehat{L})^2 + v_L$ and $\widehat{L^3} = (\widehat{L})^3 + v_L[3\widehat{L} + (v_L)^{\frac{1}{2}} S]$ where S is the skewness coefficient, allows us rewrite the condition for size-at-age r.v to rise with age (Eq. 21, which is an inequality) as

$$2\alpha \widehat{D} > \frac{v_L^*}{\widehat{L}} \left[v_L^* + (1 - \widehat{L}^2) - (v_L^*)^{\frac{1}{2}} \widehat{L} S \right]. \tag{48}$$

We now adopt two further heroic approximations, which stand or fall on the ability of the resulting estimator to match our simulation results. We first approximate $\widehat{D}$ by $D(\widehat{L})$ and second we regard the skewness of the distribution as small, so that we can set $S = 0$. The resulting approximation to the condition for size-at-age r.v., V_L^*, to increase with age is

$$\frac{2\alpha D(\widehat{L})}{(\widehat{L})^3} > V_L^* \left[V_L^* + \left(\frac{1}{(\widehat{L})^2} - 1 \right) \right] \tag{49}$$

where, from Eq. (40) the diffusion coefficient $D(\widehat{L})$ is given by

$$D(\widehat{L}) = \frac{\tau_m (1 - \widehat{L})^3}{12\alpha^2} \left[4\alpha + 3(\widehat{L} - 1) \right]. \tag{50}$$

Eq. (49), which is an inequality, gives us a cumbersome but entirely soluble quadratic for the value of size-at-age r.v. that defines the tipping point for this case. The dashed lines in Fig. 2a and c show that this tipping point implies an acceptable estimator of the measured size-at-age c.v. for cases where $L_{\min} > 1 - \alpha$.

7.3. Size-dependent mortality

To complete our investigation of the implications of von Bertalanffy growth with randomly varying growth rates, we repeat the numerical experiments shown in the lower frames of Fig. 2 with length-dependent mortality rates. In the upper frames of Fig. 3 we show two simulations with per capita mortality increasing linearly with length and in the lower two frames we show two simulations with per capita mortality decreasing linearly with length.

From Eqs. (31)–(33) and the accompanying discussion, we expect size-at-age dispersion to be increased by mortality, which increases with length and decreased by mortality, which decreases with length. Figure 3 shows that this expectation is correct. It also shows that the trajectory of size-at-age c.v rapidly 'forgets' the initial size distribution and follows an attracting trajectory similar to that shown in Fig. 2. We note that, despite the large amplitude of the assumed mortality changes, the resultant change in size-at-age c.v. is small enough to be undetectable under normal experimental protocols.

8. Discussion

8.1. Summary

In the literature on size-at-age variability (e.g. Ricker, 1958), a growth pattern in which size variability increases with age has been regarded as depensatory, while decreasing variability with age has been deemed compensatory. In this paper, we have adopted a rather stricter definition—regarding as depensatory, only those growth patterns which increase the coefficient of variation of size-at-age.

We followed Pfister and Stevens (2002) in identifying three classes of causation for changes in size-at-age variability—size dependence of growth rate, long-lived inter-individual differences in growth performance, and short-term statistically independent growth rate variability. We first developed a formal structure (Eqs. 3 and 5) within which variability arising from these causes can be discussed. We then

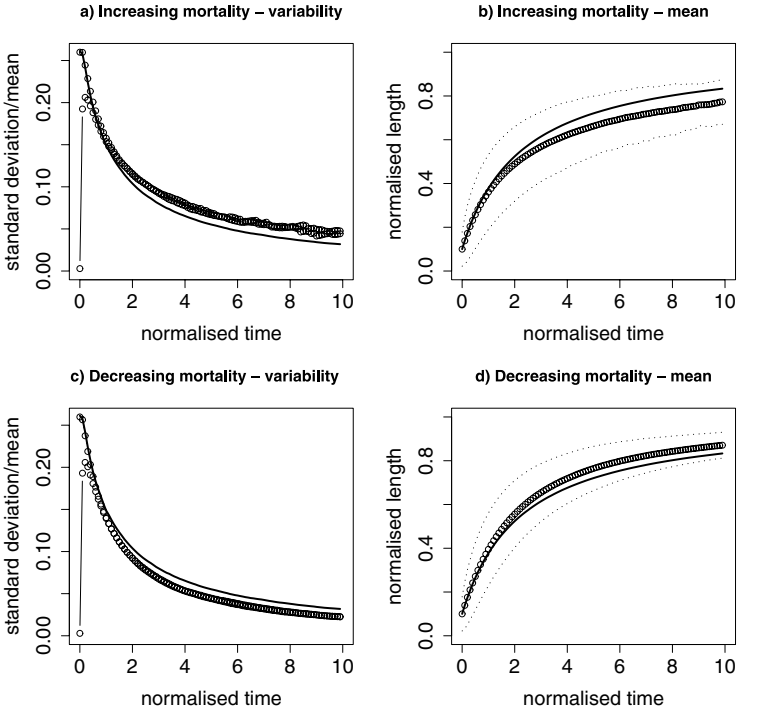

Fig. 3 Simulations of an ensemble of 50,000 individuals growing over 10 normalised time units with randomly varying growth rates and length-dependent mortality. The points in (a) show $\sqrt{V_L}$ against t for two initial conditions with $\alpha = 1$, $\tau_m = 0.05$ and $m = 10L$. One replicate has all individuals the same initial length, while the other has initial lengths spread uniformly between 0.001 and 0.19. (b) shows mean length $\pm$ 3 S.D. for the same system. The points in (c) show variability with $m = 10 - 10L$. One replicate has a delta function initial length distribution, while the other has initial lengths spread uniformly between 0.001 and 0.19. (d) shows mean length $\pm$ 3 S.D. for this simulation. The *solid lines* in (a) and (c) show $\sqrt{V_L}$ for the same system with length-independent mortality.

derived a condition for growth at a stationary state to be depensatory. In its most general form this condition is

$$\frac{G_2^*}{W_2^*} > \frac{G_1^*}{W_1^*} + \mu \tag{51}$$

where G^*, W^* and μ are defined in Eqs. (16), (7) and (32), respectively.

This rather intimidating object turns out to be much more useful than one might at first suppose. First, when the mortality rate m_i is not specifically size-dependent, we can show that μ is identically zero, thus simplifying matters considerably. In this regime we show that, whatever the nature of the stationary state size distribution(s), growth which proceeds allometrically with constant coefficients is only depensatory if the rate rises faster than proportionately with size, and is compensatory otherwise.

Second, we have shown that random growth rate variability is invariably depensatory. So, in general, is long-term individual-to-individual growth performance variation. An important exception in this latter case (see Eq. 25 and subsequent discussion) are the transient effects that occur where newly recruited individuals have size and growth rate correlated in such a way that initially larger individuals have systematically slower growth rates.

8.2. Quasi-stationary size-at-age c.v.

Where all three sources of size-at-age variation are depensatory, there is little further to say. However, in systems (such as those exhibiting von Bertalanffy growth) where size dependence implies compensation but growth rate variability is depensatory, there is the possibility that tension between these two effects will give rise to an attracting trajectory of size-at-age c.v. against age.

For the von Bertalanffy growth model, under the assumption that the scaled assimilation rate (u, defined in Eq. 35) is uniformly distributed over a range lying within [0, 1], we were able to explore this possibility analytically. To demonstrate that the existence of these quasi-stationary trajectories is not an artifact of this special (and grossly unrealistic) assumption, we now show a series of numerical experiments using more defensible forms of growth rate variation.

In Appendix D, we give a complete description of the model used, but the key feature is that the normalised assimilation rate is assumed to bear a Michaelis–Menton relationship ($u = f/(1 + f)$) to food availability f, which is itself assumed to be log-normally distributed. The resulting probability density distributions for u are shown in Fig. 4c.

The simulation results, shown in Fig. 4a and b, are clear. Under the new assumptions, and irrespective of the chosen parameters, the trajectory of size-at-age c.v. against age rapidly converges to an initial-condition-independent attractor that varies with model parameters. Although we can no longer calculate this attracting trajectory analytically, it is quite straightforward to obtain a numerical solution to the equation that results from turning Eq. (51), which is an inequality, into an equality.

The only approximation involved in this process is the assumption that size-at-age is normally distributed about its mean value. For a given mean and standard deviation, we can evaluate the two sides of the equation numerically and use standard numerical optimisation procedures to determine the value of standard deviation that causes the equation to be true for a given value of mean size (length). We see from the dashed lines in Fig. 4a and b that the relation between size-at-age c.v. and size thus determined is a good estimate of that observed—the residual discrepancy being a product of the assumption of normality in the size-at-age distribution.

8.3. Combined individual and stochastic variability

The area in which we have been able to make the least analytic progress in this paper, is where stochastic environmental variability is combined with permanent individual-to-individual differences, which are characterised in our earlier discussion as family-to-family differences. To illustrate the potential importance of these

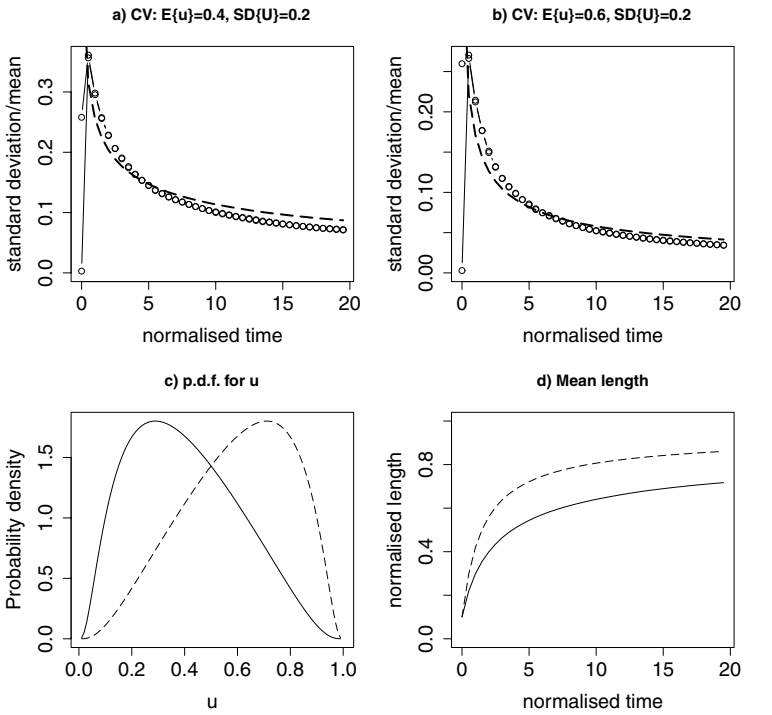

Fig. 4 Simulations of an ensemble of 10,000 individuals exhibiting ireversible von Bertalanffy growth over 20 normalised time units in increments of 0.5 time units with randomly varying growth rates $u = f/(1 + f)$ where f is lognormally distributed. The points in (a) show $\sqrt{V_L}$ against t for two initial conditions with u having a mean of 0.4 and a S.D. of 0.2. One replicate has all individuals the same initial length, while the other has initial lengths spread uniformly between 0.05 and 0.15. (b) shows two similar replicates of a system with u having mean 0.7 and standard deviation 0.2. (c) shows the probability density functions for the u in the runs in frame a (*dotted line*) and b (*dashed line*). (d) shows the mean length against time for the runs in frames a (*solid*) and b (*dashed*).

effects, we again resort to numerical experimentation with a cohort exhibiting von Bertalanffy growth. However, in this case, we assume that each family has a distinct relation between assimilation rate and food abundance, so that for family i (see Appendix D) Eq. (35) becomes

$$g_i(L, u) = \left[\frac{\xi_i}{\xi_1}u - L\right]^+, \tag{52}$$

Our experiment, whose results are shown in Fig. 5, assumes that u is uniformly distributed between 0 and 1, and that each family has a time-independent value of the ratio ξ_i/ξ_1, which is drawn from a normal distribution with mean 1 and standard deviation σ_ξ. To maximise the effect of individual-to-individual variation, we simulate a cohort containing exactly one representative of each family.

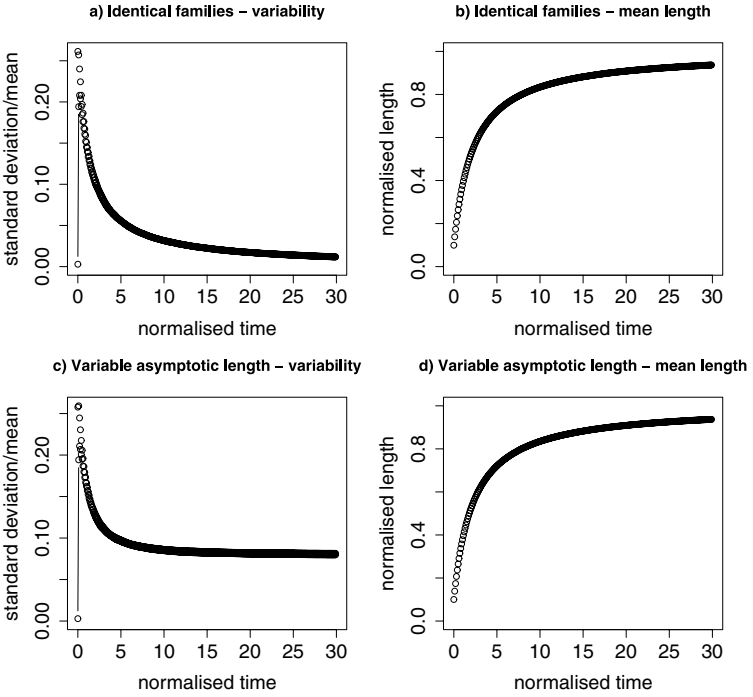

Fig. 5 Simulations of an ensemble of 10,000 individuals exhibiting ireversible von Bertalanffy growth according to Eq. (52) over 30 normalised time units in increments of 0.1 time units with randomly varying growth rates u uniformly distributed over [0, 1]. The values of normalised assimilation rate scale (ξ_i/ξ_1) are normally distributed with mean 1 and S.D. σ_ξ and each family contributes exactly one member to the cohort. Each frame shows two runs, one started with all individuals at length $L = 0.1$ and the other with individual initial sizes uniformly distributed over [0.001,0.19]. Frames (a) and (b) show the results of runs with $\sigma_\xi = 0$, and frames (c) and (d) show the results of runs with $\sigma_\xi = 0.08$.

If $\sigma_\xi = 0$ (Fig. 5a and b) we expect to reproduce the results shown in Fig. 2c and d. In particular, we notice that in this case, as we would expect from Eq. (50), the length c.v. goes to zero as the mean length approaches 1—reflecting the fact that all individuals eventually reach normalised length 1.

Although we have no formal treatment of the case where individual and stochastic variability are combined, our earlier discussion makes it quite straightforward to infer the qualitative detail of what we expect when σ_ξ is finite but not too large. When the mean length is much lower than its asymptotic value we expect most variability to be the result of stochastic growth rate variation. As the mean length approaches 1, we expect most individuals to have reached their individual asymptotic lengths and thus we expect the length variability to ever more exactly reflect the distribution of σ_ξ. Examination of Fig. 5c and d shows this to be exactly what we observe. Finally, we note that the initial-condition independence of the trajectory of length-at-age c.v. is maintained when individual-to-individual growth performance variability is an important source of population size variability.

These experiments indicate that individual-to-individual parameter variability can have very marked effects on the trajectory of size-at-age c.v. and, conversely that the asymptotic behaviour of this trajectory can provide a powerful diagnostic of the relative importance of individual-to-individual variation in some parameters as against stochastic environmental variation.

9. Conclusion

In this paper we have shown that a systematic framework can be established that allows the main sources of size-at-age variability to be described rigorously. This framework lends itself to analytic as well as numerical treatment, thus providing an alternative to the exhaustive individual-by-individual modelling studies that have been the technique of choice heretofore.

Using this framework, we have established that deterministic growth depensation (which we define as the increase of size-at-age c.v. with age) requires a growth rate which rises faster than proportionately with size, with less marked size dependence giving rise to compensatory effects in the absence of growth performance variability. Such variability, whether in the form of rapid, uncorrelated variation of realised growth, or longer-term (possibly) genetic individual-to-individual differences, is always depensatory in the long term.

Where a system exhibits a combination of deterministic compensation and growth rate variability-driven depensation, there is the possibility of a state that represents an attractive balance between these two effects—thus giving rise to an initial-condition-independent relation between size-at-age c.v. and size, which can sometimes be determined analytically, but which is always accesssible to numerical determination.

Acknowledgements

The authors wish to acknowledge helpful conversations about the dynamics of size-at-age variability with Roger Nisbet, Philip Bacon and Douglas Speirs.

Appendix

A. Continuity equation for the family age-size PDF

In this section, we derive the continuity equation for the probability density function describing the age-size distribution of a single family under the assumption that each individual's development rate parameter (γ) varies randomly. For compactness, we shall drop the family designator and denote the pdf by $P(n, a, w, t)$, the family growth function by $g(a, w, \gamma)$.

We consider a time step dt during which we regard each individual's value of γ as an independent constant drawn from a family-specific distribution characterised by a probability density function $\phi(\gamma)$. We note that all individuals with a given

value of γ in a volume element $\mathrm{d}V \equiv \mathrm{d}n\,\mathrm{d}a\,nw$ at (n, a, w) at time t must be the survivors of those found at time $t - \mathrm{d}t$ in a volume

$$\mathrm{d}V' = \mathrm{d}n\left[1 + \frac{\partial(nm)}{\partial n}\,\mathrm{d}t\right]\mathrm{d}w\left[1 - \frac{\partial g}{\partial w}\mathrm{d}t\right]\mathrm{d}a \tag{A.1}$$

at $(n + mn\,\mathrm{d}t, w - g\,\mathrm{d}t, a - \mathrm{d}t)$.

The proportion of the family members in $\mathrm{d}V$ who have parameters in $\gamma \to \gamma + \mathrm{d}\gamma$ is $\phi(\gamma)\mathrm{d}\gamma$. Hence we can see that the probability density in $\mathrm{d}V$ at time t is related to the probability density function at time $t - \mathrm{d}t$ by

$$P(n, w, a, t)\mathrm{d}V = \int_{-\infty}^{\infty} \phi(\gamma)\,P(n + mn\,\mathrm{d}t, w - g\,\mathrm{d}t, a - \mathrm{d}t, t - \mathrm{d}t)\,\mathrm{d}V'\mathrm{d}\gamma. \tag{A.2}$$

Expanding the source density to second order in $\mathrm{d}t$, collecting up terms and dividing through by $\mathrm{d}n\,\mathrm{d}w\,\mathrm{d}a\,\mathrm{d}t$ shows that

$$\frac{\partial P}{\partial t} + \frac{\partial P}{\partial a} - \frac{\partial(mnP)}{\partial n} + \int_{-\infty}^{\infty} \phi\frac{\partial}{\partial w}\left[gP - \frac{g^2\mathrm{d}t}{2}\frac{\partial P}{\partial w}\right]\mathrm{d}\gamma + O(\mathrm{d}t) = 0. \tag{A.3}$$

Recalling that only the development rate function (g) depends explicitly on γ, and using an overbar to denote the expectation of any quantity depending on γ over the probability density function ϕ allows us to rewrite this as

$$\frac{\partial P}{\partial t} + \frac{\partial P}{\partial a} - \frac{\partial(mnP)}{\partial n} + \frac{\partial}{\partial w}\left[\overline{g}P - \frac{\overline{g^2}\,\mathrm{d}t}{2}\frac{\partial P}{\partial w}\right] + O(\mathrm{d}t) = 0. \tag{A.4}$$

The reason for retaining a term of $O(\mathrm{d}t)$ in the square brackets is that we assume that the noise process driving variation in γ is 'white'—implying that it has a constant power spectral density ($2D$) over all possible frequencies. This, in turn, implies that while the mean of the process will remain finite as $\mathrm{d}t \to 0$, the variance, $\sigma_g^2 = 2D\,\mathrm{d}t^{-1}$, will go to ∞ as $\mathrm{d}t^{-1}$ (Nisbet and Gurney, 2003).

Hence, recalling that $\sigma_g^2 = \overline{g^2} - (\overline{g})^2$, we see that as we proceed to the limit of very small time increments, our dynamic equation for the family age-size probability density function becomes

$$\frac{\partial P}{\partial t} + \frac{\partial P}{\partial a} - \frac{\partial(mnP)}{\partial n} + \frac{\partial}{\partial w}\left[\overline{g}P - D\frac{\partial P}{\partial w}\right] = 0. \tag{A.5}$$

B. Double sum of a function

We consider a function $\phi_{i,j}$, which is defined for $i, j \in [1, N]$. Our interest is in the sum of ϕ over its entire domain, that is in

$$S \equiv \sum_i \sum_j \phi_{i,j}. \tag{B.1}$$

Clearly, we can rewrite S as

$$S = \sum_i \sum_{j<i} \phi_{ij} + \sum_i \sum_{j \geq i} \phi_{ij}. \tag{B.2}$$

By performing the second of these double summations in reverse order we get

$$S = \sum_i \sum_{j<i} \phi_{ij} + \sum_j \sum_{i<j} \phi_{ij}. \tag{B.3}$$

Finally, we interchange i and j in the second term, and amalgamate the resulting sums, to obtain

$$S = \sum_i \sum_{j<i} [\phi_{ij} + \phi_{j,i}]. \tag{B.4}$$

C. Double integral of a function

We consider a function $\phi(x, y)$. Our interest is in the double integral

$$I \equiv \int_0^\infty \int_0^\infty \phi(x, y)\, \mathrm{d}x\, \mathrm{d}y. \tag{C.1}$$

Clearly we can rewrite I as

$$I = \int_0^\infty \int_0^y \phi(x, y)\, \mathrm{d}x\, \mathrm{d}y + \int_0^\infty \int_y^\infty \phi_(x, y)\, \mathrm{d}x\, \mathrm{d}y. \tag{C.2}$$

By performing the second of these double integrals in reverse order, I becomes

$$I = \int_0^\infty \int_0^y \phi(x, y)\, \mathrm{d}x\, \mathrm{d}y + \int_0^\infty \int_0^x \phi_(x, y)\, \mathrm{d}y\, \mathrm{d}x. \tag{C.3}$$

Finally, interchanging x and y in the second term, yields

$$I = \int_0^\infty \int_0^y [\phi(x, y) + \phi(y, x)]\, \mathrm{d}x\, \mathrm{d}y. \tag{C.4}$$

D. The von Bertalanffy growth model

One standard derivation of the von Bertalanffy growth model asserts that the weight and length of an animal are related by

$$W' = \chi L'^3, \tag{D.1}$$

its basal metabolic costs are proportional to weight (with constant of proportionality b') and its uptake rate in the presence of food at density f' is proportional

to its cross-sectional area (L'^2) and to a Michaelis–Menton factor related to food density (f'). Thus

$$u' = \frac{\xi L'^2 f'}{f_H + f'}. \tag{D.2}$$

Hence, assuming that it is reproductively inactive, so that somatic growth and basal metabolism are its only expenditures, the rate of change of weight is

$$\frac{\mathrm{d}W'}{\mathrm{d}t'} = 3\chi L'^2 \frac{\mathrm{d}L'}{\mathrm{d}t'} = \frac{\xi L'^2 f'}{f'_H + f'} - b'\chi L'^3. \tag{D.3}$$

If we define $t = b't'/3$, $L = b'\chi L'/\xi$ and $f = f'/f'_H$, this reduces to

$$\frac{\mathrm{d}L}{\mathrm{d}t} = u - L, \quad \text{where} \quad u = \frac{f}{1+f}. \tag{D.4}$$

If, in addition we assert that when $u < L$ the animal cannot shrink, but instead retains its existing length, then the model becomes

$$\frac{\mathrm{d}L}{\mathrm{d}t} = [u - L]^+, \quad \text{where} \quad [x]^+ = \max(0, x). \tag{D.5}$$

To simulate this growth process, we assume that over some time increment $t \to t + \mathrm{d}t$, u remains constant at a value u_t, so that

$$L_{t+\mathrm{d}t} = \begin{cases} u_t + (L_t - u_t)\,\mathrm{e}^{-\mathrm{d}t}, & \text{if } u_t > L_t \\ L_t, & \text{otherwise.} \end{cases} \tag{D.6}$$

We note that, if the normalised food density f is lognormally distributed with mean m and standard deviation s, that is

$$\phi_f = N_L(f, m, s), \tag{D.7}$$

then u is distributed over $[0, 1]$ with a probability density function

$$\phi(u) = \frac{1}{(1-u)^2}\phi_f\left(\frac{u}{1-u}, m, s\right). \tag{D.8}$$

In the case where we wish to represent multiple families, each with a distinct value of the assimilation rate scale ξ_i, the above discussion repeats almost exactly except that we need to choose the value for a single family (say $i = 1$) to define our scaling, that is we define $L = b'\chi L'/\xi_1$. Hence, our final model for family i is

$$\frac{\mathrm{d}L_i}{\mathrm{d}t} = \frac{\xi_i}{\xi_0}u - L_i, \quad \text{where} \quad u = \frac{f}{1+f}. \tag{D.9}$$

References

Bardos, D.C., 2005. Probabilistic Gompertz model of irreversible growth. Bull. Math. Biol. 67, 529–545.
Brunkow, P.E., Collins, J.P., 1998. Group size structure affects patterns of aggression in larval salamanders. Behav. Ecol. 9, 508–514.
DeAngelis, D.L., Huston, M.A., 1987. Effects of growth rates in models of size distribution formation in plants and animals. Ecol. Modell. 36, 119–137.
DeAngelis, D.L., Cox, D.C., Coutant, C.C., 1979. Cannibalism and size dispersal in young of the year large-mouth bass: Experiments and model. Ecol. Modell. 24, 21–41.
de Roos, A.M., Diekmann, O., Metz, J.A.J., 1992. Studying the dynamics of structured population models: A versatile technique and its application to Daphnia population dynamics. Am. Nat. 139, 123–147.
Fujiwara, M., Kendall, B.E., Nisbet, R.M., 2005. Growth autocorrelation and animal size variation. Ecol. Lett. 7, 106–113.
Fujiwara, M., Kendall, B.E., Nisbet, R.M., Bennett, W.A., 2005. Analysis of size trajectory data using an energetic-based growth model. Ecology 86, 1441–1451.
Gompertz, B., 1825. On the nature of the function expressive of the law of human mortality, and on a new mode of determining the value of life contingencies. Philos. Trans. R. Soc. Lond. 115, 513–585.
Imsland, A.K., Nilsen, T., Folkvord, A., 1998. Stochastic simulation of size variation in Turbot: Possible causes analysed with an individual-based model. J. Fish. Biol. 53, 237–258.
Marteinsdottir, G., Begg, G., 2002. Essential relationships incorporating influences of age, size and condition on variables required for estimation of reproductive potential in Atlantic cod (Gadus morhus) stocks. Mar. Ecol. Prog. Ser. 235, 235–256.
Nisbet, R.M., Gurney, W.S.C., 2003. Modelling Fluctuating Populations. Blackburn, Caldwell, NJ, pp. 243–250.
Pfister, C.A., Stevens, F.R., 2002. The genesis of size variability in plants and animals. Ecology 83, 59–72.
Pfister, C.A., Peacor, S.D., 2003. Variable performance of individuals: The role of population density and endogenously formed landscape heterogeneity. J. Anim. Ecol. 72, 725–735.
Ricker, W.E., 1958. Handbook of Computations for Biological Statistics of Fish Populations. Fisheries Research Board of Canada, Nanaimo, BC, Canada. Bulletin 119.
Rose, G., 2004. Reconciling overfishing and climate changes with stock dynamics of Atlantic cod (Gadus morhua) over 500 years. Can. J. Fish. Aquat. Sci. 61, 1553–1557.
Sebens, K.P., 1987. The ecology of indeterminate growth. Ann. Rev. Ecol. Syst. 18, 371–407.
von Bertalanffy, L., 1938. A quantitative theory of organic growth (inquiries on growth laws) II. Hum. Biol. 10, 181–213.
von Foerster, H., 1959. Some remarks on changing populations. In: Stohlman, F. (Ed.), The Kinetics of Cellular Proliferation. Grune and Stratton, New York.
Wootton, J.T. 1992. Indirect effects, prey susceptibility and habitat selection: Impacts of birds on limpets and algae. Ecology 73, 981–991.